Desai, R. W., J. W. Rachow, and D. C. Timm, "Collision Breeding: A Function of Crystal Moments and Degree of Mixing," *AIChE J.*, **20**, 43 (1974).
Garret, P. E., "Industrial Crystallization: Influence of Chemical Environment," *Brit. Chem. Eng.*, **4**, 673 (1959).
Larson, M. A., D. C. Timm, and P. R. Wolff, "Effect of Suspension Density on Crystal Size Distribution," *AIChE J. 14*, **3**, 448 (1968).
Liu, Y. A., and G. D. Botsaris, "Impurity Effects in Continuous-Flow Mixed Suspension Crystallizer," *AIChE J.* 3, **19**, 510 (1973).
Mason, R. E. A., and R. F. Strickland-Constable, "Breeding of Crystal Nuclei," *Trans. Faraday Society*, **62**, 455 (1969).
Michaels, A. S., and F. W. Tausch, Jr., "Modification of Growth Rate and Habit of Adipic Acid Crystals with Surfactants," *J. of Phys. Chem.*, **65**, 1730 (1961).
Ness, J. N., and E. T. White, "Collision Nucleation in a Agitated Crystallizer," 77th AIChE Nat. Meeting, Pittsburgh, PA (June, 1974).
Randolph, A. D., and K. Rajagopal, "Direct Measurement of Crystal Nucleation and Growth Rate Kinetics in a Backmixed Crystal Slurry," *I & EC Fundamentals*, **9**, 165 (1970).
Randolph, A. D., and M. D. Cise, "Nucleation Kinetics of Potassium Sulphate-Water System," *AIChE J.*, **18**, 798 (1972).
Randolph, A. D., and S. Koontz, "Effects of Habit and Nucleation Modifiers in Crystallization of Sodium Tetraborate Decahydrate (Borax)," 69th AIChE Annual Meeting, Chicago (1976).
Shadman, F., and A. D. Randolph, "Nucleation and Growth Rate of Ammonium Chloride in Organic Media: Development of an On-Line Measurement Technique," *AIChE J.*, **24**, 782 (1978).
Shor, S. M., and M. A. Larson, "Effect of Additives on Crystallization Kinetics," *AIChE Symp. Ser.* No. 110, **67**, 32 (1971).

Manuscript received January 8, 1980; revision received May 13, and accepted May 20, 1980.

Drop Size and Continuous-Phase Mass Transfer in Agitated Vessels

Continuous-phase mass transfer coefficients and drop sizes in agitated vessels are correlated with operating variables and physical properties of liquid-liquid systems. In formulating mass transfer coefficients, a realistic mechanism has been developed, involving periodically varying rates of surface renewal associated with droplet circulation through varying degrees of turbulence around the vessel. Relationships are obtained for optimized design and scale-up.

A. H. P. SKELLAND
and
JAI MOON LEE
Chemical Engineering Department
University of Kentucky
Lexington, Kentucky 40506

SCOPE

The rate of mass transfer between two immiscible liquids in mixing vessels depends on the concentration difference, the interfacial area, and the mass transfer coefficient. The comprehensive correlation of mass transfer coefficients and interfacial areas are therefore essential for the optimized design and scale-up of such equipment.

Schindler and Treybal (1968) and Keey and Glen (1969) studied liquid-liquid mass transfer rates in agitated vessels. Both investigations were confined to single systems, so that comprehensive correlations over a range of physical properties were not established.

The objects of this research are to measure and correlate such continuous-phase mass transfer coefficients and the corresponding drop sizes in the presence of mass transfer. Relationships for optimized design and scale-up will then be formulated.

CONCLUSIONS AND SIGNIFICANCE

The continuous-phase mass transfer coefficient has been correlated and separate correlations for high and low interfacial tension systems have also been attempted for a better fit of the data.

Comparison between our correlation for k_c and expressions derived from the penetration theory with Kolmogoroff's time scale and from turbulent boundary layer theory show significant differences between the exponents on any given variable, suggesting the need for a new model. Accordingly, a theory based on a periodically varying rate of surface renewal has been developed and the average rate of surface renewal s_a in this theory has been correlated.

Droplet size was determined from photographs of the dispersion taken through a plane glass water pocket. A correlation was obtained for the Sauter-mean drop diameter when about 50% of the possible mass transfer had occurred; this was chosen as an average value during batch operation.

These correlations have been used to develop relationships for optimized design and scale-up.

This study included five liquid-liquid systems, two sizes of six-flat-blade turbines, two vessel diameters, two principal liquid heights (T = H), impeller speeds between 3 and 8 rps, and dispersed-phase volume fractions between 0.03 and 0.09.

Jai Moon Lee is with the Chemical Engineering Department, Cleveland State University, Cleveland, Ohio 44115
A. H. P. Skelland is now with the Chemical Engineering Department, Georgia Institute of Technology, Atlanta, Georgia 30332

0001-1541-81-4235-0099- $02.00.

Mass Transfer Coefficients in Agitated Vessels

Schindler and Treybal (1968) measured the area-free, continuous-phase mass transfer coefficients for continuous flow of ethyl acetate (dispersed) and water (continuous) in a baffled vessel, agitated with flat-blade turbines. The specific interfacial area was determined by a light transmission technique. An unsteady-state diffusion model for a continuous-phase stagnant shell around each drop was employed to deduce the expression

$$k_c = \frac{\mathscr{D}_A R'}{(R' - r_p) r_p} + \sum_{n=1}^{\infty} \frac{2(R' - r_p)}{n^2 \pi^2 \theta_c} \left[1 - \exp \frac{-n^2 \pi^2 \mathscr{D}_A \theta_c}{(R' - r_p)^2} \right] \quad (1)$$

The first term on the right is a steady-state coefficient, the second a transient term. However, the authors stated that the derivation of the above equation was unrealistic in that it assumed only molecular diffusion, no circulation of the fluid around the drop, no drop oscillation, and no slip or fluctuating velocities. But, from the above equation, they inferred a more general expression:

$$k_c = k_s + \text{const.} \ (\mathscr{D}_A/\theta_c)^{0.5} \quad (2)$$

The steady-state k_s was tentatively recommended to be estimated by Harriott's (1962) correlation, in which case the constant in Eq. 2 was found to be 3.94.

Keey and Glen (1969) investigated the continuous-phase mass transfer coefficient for the system iso-octane/o-nitrophenol (solute)/water in continuously operated baffled vessels, agitated with various sizes of six-blade paddles. An expression was derived on the assumption that the drops were surrounded by turbulent boundary layers as follows:

$$N_{Sh} \propto N_{Re}^{1.375} N_{Sc}^{\frac{1}{2}} \quad (3)$$

and the general correlation of their data is:

$$N_{Sh} = 8.92 \times 10^{-4} N_{Re}^{1.36} T^{-0.5} d_I^{0.36} - 336 \quad (4)$$
$$10^4 < N_{Re} < 10^5$$

Studies of solids or gases dispersed in liquids have been more extensive than those of liquid-liquid systems (Sherwood et al., 1975a; Prasher and Wills, 1973; Calderbank and Moo-Young, 1961; Sideman et al., 1966). Prasher and Wills (1973) examined the applicability of Lamont's eddy cell model (Lamont and Scott, 1970) to gas-liquid transfer in turbulent flow in an agitated vessel. According to this model, the very small scales of turbulent motion in the equilibrium range are considered to be controlling the mass transfer process. The following relationship is predicted for the mass transfer coefficient at a free interface:

$$k_c \propto N_{Sc}^{-1/2} (\epsilon \nu)^{1/4} \quad (5)$$

Correlations for Sauter-Mean Droplet Diameter in Agitated Vessels

Some correlations for liquid-liquid systems may be noted briefly as follows. Thornton and Bouyatiotis (1963) recorded the droplet-size distributions photographically in a fully baffled vessel. Their correlation is

$$d_{32} = d_{32}^o + \phi \left(\frac{\sigma^2}{\mu_c^2 g} \right) \left(\frac{\Delta\rho\sigma^3}{\mu_c^4 g} \right)^{-0.78} \left(\frac{\Delta\rho}{\rho_c} \right)^{0.89} \quad (6)$$

The drop size at substantially zero holdup, d_{32}^o, was correlated as

$$\frac{(d_{32}^o)^3 \rho_c^2 g}{\mu_c^2} = 31.2 \left(\frac{P_v^3}{\rho_c^2 \mu_c g^4} \right)^{-0.32} \left(\frac{\rho_c \sigma^3}{\mu_c^4 g} \right)^{0.14} \quad (7)$$

Keey and Glen (1969) reported that a diameter-frequency plot showed the droplet sizes during mass transfer to have a logarithmic-normal distribution. Their diameters were fitted by:

$$d_{32} = 3.165 \times 10^{-4} \frac{d_I^{2/5}}{(N d_I)^{6/5}} \cdot \left(\frac{T}{d_I} \right)^{6/5} \quad (8)$$

Schindler and Treybal (1968) used a low interfacial tension system and reported that the drop sizes were smallest in the impeller stream and largest in the regions farthest from the impeller, because of coalescence in regions of relatively low turbulence intensity. No correlation was presented.

Sprow (1967) determined the distribution of drop diameters near a turbine impeller in a dilute iso-octane and salt water emulsion, using an electronic particle counter. His correlation is

$$d_{32} = 0.0524 \ \sigma^{3/5} \rho_c^{-3/5} N^{-6/5} d_I^{4/5} \quad (9)$$

for

$$\phi < 0.015$$

Mlynek and Resnick's (1972) dispersions were sampled in a special trap and immediately encapsulated by a polymer film. They used water and a mixture of iso-octane and carbon tetrachloride with density close to that of water. For this system, which has low mutual solubility and high interfacial tension, there was no dependency of drop size on location in the vessel. They concluded that the coalescence rate is low compared to the circulation time, and they give the following correlation:

$$\frac{d_{32}}{d_I} = 0.058(1 + 5.4\phi) N_{We}^{-0.6} \quad (10)$$

Coulaloglou and Tavlarides (1976) tabulated various published correlations for drop size. They also measured size distributions and mixing frequencies in a turbulently agitated flow vessel with a flash photomicrograhpic method and a dye-light transmittance technique. The correlation they obtained is

$$\frac{d_{32}}{d_I} = 0.081(1 + 4.47\phi) N_{We}^{-0.6} \quad (11)$$

The existing correlations were made after the establishment of steady-state conditions. Since most mass transfer takes place before the drop size becomes steady, a drop size correlation is needed for short residence times and *during* mass transfer. This will facilitate the evaluation of area-free mass transfer coefficients in batch processes. The development of such a correlation is one objective of this study.

THEORETICAL DEVELOPMENT

Periodically Varying Rate of Surface Renewal

Several different mechanisms have been proposed to describe conditions near the interface between two phases. These are reviewed by Sherwood et al. (1975b), Skelland (1974b), and Treybal (1968a).

According to Danckwert's (1951) surface renewal theory, the fractional rate of surface renewal, s, is assumed to remain constant. This may not hold for a droplet of the dispersed phase circulating around an agitated vessel, because of different degrees of turbulence at various locations in the vessel.

The circulation pattern in an agitated vessel with a centrally located six-blade turbine will be somewhat as sketched in Figure 1(a). The turbulence will be greatest near the impeller (1), least in the "corners" of the vessel (3), and of intermediate strength in regions between these locations (2 and 4). The fractional rate of surface renewal in the continuous phase, s, near each drop of dispersed phase will be correspondingly greatest near the impeller, least in the vessel "corners," and of average levels in the regions in between. Schematically, the situation can be shown as Figure 1(b), where t_c is the average circulation time of the droplets around the vessel.

The model with periodically varying rate of surface renewal

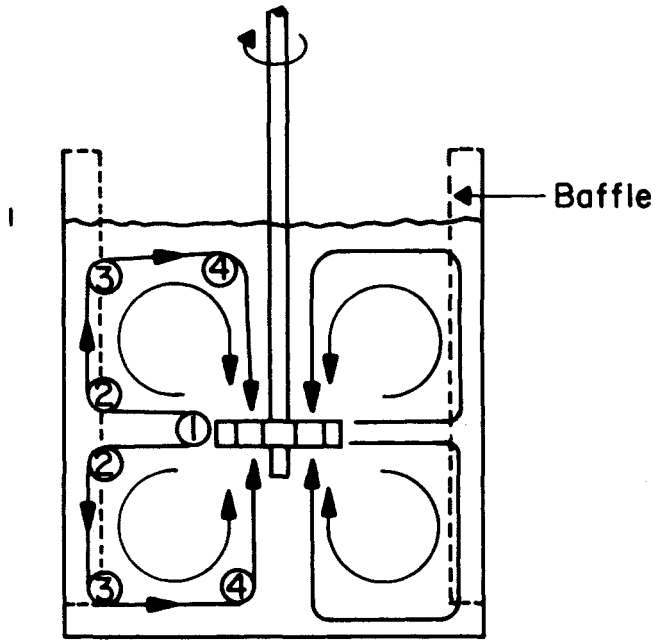

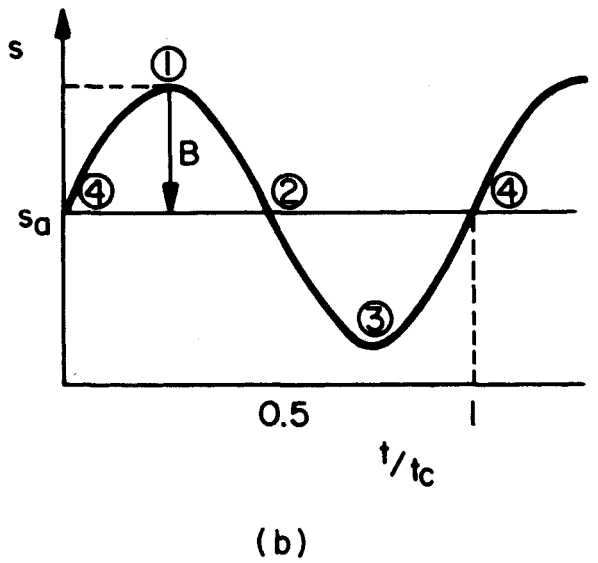

Figure 1. (a) circulation pattern for a six-flat-blade turbine; (b) periodically varying rate of surface renewal in continuous-phase adjacent to droplets.

pictures eddies in the continuous phase travelling to and from the surface of each droplet. The feasibility of this concept depends on the ratio of drop size to eddy size. Treybal (1968b) states that the size of droplets is usually in the range of 0.1 to 1 mm in diameter, depending on the liquid properties and the agitation power, and this was the case in this research. Calderbank (1967) shows that typically the scale of the smallest eddies is 25 microns. Therefore the ratio of droplet diameter to eddy size d_p/l is between 4 and 40, showing that the droplets are significantly larger than the smallest eddies. Thus, the physical picture for the proposed model is reasonable.

Danckwerts (1951) defined a surface age distribution function $\phi(t)$, such that the fraction of surface with ages between t and $t + dt$ is $\phi(t)dt$. Following Danckwerts' procedure:

$$\frac{d\phi(t)}{dt} = -s\phi(t) \tag{12}$$

In accordance with Figure 1(b), let

$$s = s_a + B \sin\frac{2\pi t}{t_c} \tag{13}$$

where the average rate of surface renewal, s_a, is larger than B, so that s may have only positive values. Substituting Eq. 13 into Eq. 12 and solving for $\phi(t)$ gives

$$\phi(t) = C \exp\left(-s_a t + \frac{Bt_c}{2\pi}\cos\frac{2\pi t}{t_c}\right) \tag{14}$$

where C can be obtained by using the condition that $\int_0^\infty \phi(t)dt = 1$. Thus,

$$\frac{1}{C} = \int_0^\infty \exp\left(-s_a t + \frac{Bt_c}{2\pi}\cos\frac{2\pi t}{t_c}\right)dt \tag{15}$$

By performing the integration (Lee, 1978),

$$\frac{1}{C} = \sum_{l=0}^{\infty}\sum_{p=0}^{l}\frac{(Bt_c/2\pi)^l}{2^l p!(l-p)![s_a - (2\pi/t_c)(l-2p)i]} \tag{16}$$

The instantaneous rate of transfer from the surface for a given element, derived by Higbie (1935), is

$$n_{Ao} = (\rho_A^* - \rho_{A\infty})\left(\frac{\mathscr{D}}{\pi t}\right)^{\frac{1}{2}} \tag{17}$$

Thus, for all elements with ages between t and $t + dt$, the instantaneous transfer rate is

$$\phi(t)(\rho_A^* - \rho_{A\infty})\left(\frac{\mathscr{D}}{\pi t}\right)^{\frac{1}{2}} dt$$

The flux of component A from a surface having elements with ages distributed over the range $0 < t < \infty$ is therefore

$$(n_{Ao})_{av.} = (\rho_A^* - \rho_{A\infty})\int_0^\infty \phi(t)\left(\frac{\mathscr{D}}{\pi t}\right)^{\frac{1}{2}} dt \tag{18}$$

Since $k = (n_{Ao})_{av}/(\rho_A^* - \rho_{A\infty})$,

$$k = \int_0^\infty \phi(t)\left(\frac{\mathscr{D}}{\pi t}\right)^{\frac{1}{2}} dt \tag{19}$$

Combining Eqs. 14, 16, and 19 and integrating (Lee, 1978),

$$\frac{k}{\sqrt{\mathscr{D}}} = \frac{\sum_{l=0}^{\infty}\sum_{p=0}^{l}\frac{(Bt_c/2\pi)^l}{2^l p!(l-p)![s_a - (2\pi/t_c)(l-2p)i]^{\frac{1}{2}}}}{\sum_{l=0}^{\infty}\sum_{p=0}^{l}\frac{(Bt_c/2\pi)^l}{2^l p!(l-p)![s_a - (2\pi/t_c)(l-2p)i]}} \tag{20}$$

which predicts that the mass transfer coefficient is directly proportional to the square root of the molecular diffusivity. Tables 1(a) and 1(b) are the results of the first fifteen terms of the summation in Eq. 20, where x denotes B/s_a. Since convergence is rapid, the first fifteen terms gave good results to three significant figures.

Mass transfer coefficients can therefore be obtained from Eq. 20 or Table 1. The circulation time, t_c, can be estimated for a baffled vessel with a turbine impeller from Holmes et al. (1964),

$$t_c = 0.85\frac{1}{N}\left(\frac{d_I}{T}\right)^2, \quad N_{Re} > 2 \times 10^4 \tag{21}$$

The value of $x = B/s_a$ can be estimated by the expression (Lee, 1978):

$$x = \frac{k_1 - k_3(d_I/T)}{k_1 + k_3(d_I/T)} \tag{22}$$

where k_1 and k_3 are $\overline{U}_1/\pi d_I N$ and $(\overline{U}_3/\pi d_I N)(T/d_I)$, respectively,

TABLE 1(A). VALUES OF $k/\sqrt{\mathscr{D}}$ AS A FUNCTION OF x, t_c, AND s_a.

X	TC	SA									
		1.000	2.000	3.000	4.000	5.000	6.000	7.000	8.000	9.000	10.000
0.200	0.200	1.001	1.417	1.739	2.013	2.256	2.478	2.683	2.876	3.059	3.234
0.200	0.400	1.002	1.423	1.752	2.034	2.287	2.518	2.733	2.935	3.124	3.304
0.200	0.600	1.004	1.430	1.766	2.056	2.315	2.551	2.768	2.969	3.156	3.330
0.200	1.000	1.009	1.446	1.793	2.090	2.349	2.580	2.788	2.978	3.154	3.319
0.200	2.000	1.023	1.478	1.824	2.106	2.347	2.561	2.755	2.936	3.105	3.264
0.400	0.200	1.002	1.421	1.747	2.026	2.276	2.506	2.721	2.925	3.119	3.306
0.400	0.400	1.005	1.432	1.772	2.068	2.338	2.587	2.821	3.041	3.248	3.443
0.400	0.600	1.008	1.447	1.801	2.112	2.394	2.652	2.887	3.104	3.303	3.487
0.400	1.000	1.018	1.478	1.855	2.177	2.457	2.701	2.917	3.111	3.289	3.454
0.400	2.000	1.045	1.540	1.910	2.200	2.443	2.655	2.848	3.027	3.193	3.351
0.500	0.200	1.002	1.422	1.750	2.032	2.286	2.520	2.740	2.949	3.150	3.342
0.500	0.400	1.006	1.437	1.782	2.086	2.363	2.622	2.865	3.093	3.308	3.511
0.500	0.600	1.011	1.455	1.818	2.141	2.434	2.701	2.946	3.169	3.373	3.561
0.500	1.000	1.022	1.495	1.885	2.220	2.509	2.758	2.977	3.172	3.351	3.515
0.500	2.000	1.057	1.570	1.950	2.243	2.486	2.698	2.890	3.067	3.233	3.390
0.600	0.200	1.002	1.424	1.754	2.039	2.296	2.535	2.760	2.974	3.180	3.379
0.600	0.400	1.007	1.442	1.792	2.103	2.389	2.657	2.908	3.146	3.369	3.578
0.600	0.600	1.013	1.463	1.836	2.169	2.473	2.750	3.003	3.232	3.441	3.632
0.600	1.000	1.027	1.511	1.916	2.263	2.559	2.813	3.034	3.230	3.408	3.573
0.600	2.000	1.068	1.600	1.989	2.284	2.526	2.738	2.929	3.106	3.271	3.427
0.650	0.200	1.003	1.425	1.756	2.042	2.301	2.542	2.769	2.986	3.195	3.397
0.650	0.400	1.007	1.444	1.797	2.112	2.402	2.674	2.930	3.172	3.398	3.611
0.650	0.600	1.014	1.468	1.845	2.183	2.493	2.775	3.031	3.263	3.474	3.666
0.650	1.000	1.029	1.519	1.931	2.284	2.584	2.840	3.061	3.258	3.436	3.600
0.650	2.000	1.074	1.615	2.008	2.304	2.545	2.757	2.948	3.124	3.289	3.445
0.700	0.200	1.003	1.426	1.758	2.045	2.306	2.549	2.779	2.999	3.210	3.415
0.700	0.400	1.008	1.446	1.802	2.120	2.415	2.691	2.952	3.197	3.428	3.644
0.700	0.600	1.015	1.472	1.854	2.197	2.512	2.799	3.059	3.294	3.506	3.700
0.700	1.000	1.031	1.527	1.946	2.305	2.608	2.866	3.088	3.285	3.463	3.626
0.700	2.000	1.080	1.630	2.026	2.323	2.564	2.775	2.966	3.142	3.307	3.462
0.800	0.200	1.003	1.427	1.761	2.052	2.316	2.563	2.798	3.023	3.241	3.452
0.800	0.400	1.009	1.451	1.813	2.138	2.441	2.726	2.995	3.249	3.487	3.709
0.800	0.600	1.017	1.480	1.871	2.226	2.551	2.847	3.114	3.354	3.570	3.765
0.800	1.000	1.036	1.544	1.976	2.345	2.656	2.916	3.140	3.336	3.514	3.677
0.800	2.000	1.092	1.658	2.062	2.359	2.600	2.810	3.000	3.176	3.340	3.496
0.900	0.200	1.004	1.429	1.765	2.058	2.327	2.578	2.818	3.048	3.271	3.488
0.900	0.400	1.010	1.456	1.823	2.155	2.467	2.761	3.039	3.300	3.544	3.772
0.900	0.600	1.019	1.488	1.889	2.254	2.589	2.894	3.168	3.412	3.631	3.827
0.900	1.000	1.040	1.560	2.006	2.386	2.701	2.965	3.189	3.385	3.562	3.725
0.900	2.000	1.103	1.687	2.096	2.394	2.634	2.844	3.033	3.209	3.373	3.527
1.000	0.200	1.004	1.431	1.769	2.065	2.337	2.593	2.837	3.073	3.302	3.525
1.000	0.400	1.012	1.460	1.833	2.173	2.492	2.795	3.081	3.350	3.601	3.834
1.000	0.600	1.021	1.497	1.906	2.282	2.628	2.940	3.220	3.468	3.689	3.887
1.000	1.000	1.045	1.576	2.035	2.425	2.746	3.011	3.235	3.432	3.608	3.771
1.000	2.000	1.115	1.715	2.129	2.427	2.666	2.875	3.065	3.240	3.403	3.558

and can be assessed from the flow velocity data of Nagata et al. (1959), or McCabe and Smith (1976). The quantities $\overline{U}_1$ and $\overline{U}_3$ are the maximum and minimum flow velocities in the vessel.

Using the velocity distribution patterns for six-bladed turbines given by Nagata et al. (1959), $k_1 \doteq 0.78$ and $k_3 \doteq 0.43$. Alternative estimates from less extensive velocity distribution data (McCabe and Smith, 1976) are $k_1 \doteq 0.7$ and $k_3 \doteq 0.3$.

Mass Transfer Coefficient Correlation Based on Penetration Theory with Kolmogoroff's Time Scale

The universal equilibrium range in a turbulent fluid is usually defined as the range of wave numbers associated with small and statistically steady eddies that are responsible for the viscous dissipation of energy. Kolmogoroff's theory postulates that the eddies in this equilibrium state depend only on the rate of energy dissipation, ϵ, and the kinematic viscosity, ν (Hinze, 1975 and Brodkey, 1967). From dimensional reasoning, Kolmogoroff's length, velocity, and time scales are defined as follows (Hinze, 1975):

$$\text{length scale:} \quad \eta = \left(\frac{\nu^3}{\epsilon}\right)^{1/4} \tag{23}$$

$$\text{velocity scale:} \quad v = (\nu\epsilon)^{1/4} \tag{24}$$

$$\text{time scale:} \quad \tau_k = \left(\frac{\nu}{\epsilon}\right)^{1/2} \tag{25}$$

These scales have been used successfully with forms of the penetration theory in correlating the following phenomena:

1) mass transfer in falling wavy liquid films in turbulent flow (Banerjee et al., 1968),

2) oxygenation of naturally flowing rivers (Nadkarni and Russell, 1973),

3) absorption of gases in liquids in agitated vessels (Prasher and Wills, 1973), and

4) drop size in liquid-liquid dispersions (Calderbank, 1967).

Kolmogoroff's time scale will therefore be used—with the penetration theory—in an attempt to predict a form for k_c.

Thus, from Higbie's (1935) penetration theory,

$$k = 2\sqrt{\frac{\mathscr{D}}{\pi t_c}} \tag{26}$$

where t_c will be taken to be given by τ_k, or

$$t_c = (\nu/\epsilon)^{1/2} \tag{27}$$

TABLE 1(B). VALUES OF $k/\sqrt{\mathscr{D}}$ AS A FUNCTION OF x, t_c, AND s_a.

X	TC	SA									
		20.000	30.000	40.000	50.000	60.000	70.000	80.000	90.000	100.000	200.000
0.200	0.200	4.672	5.768	6.659	7.421	8.097	8.713	9.283	9.817	10.322	14.396
0.200	0.400	4.709	5.726	6.564	7.299	7.962	8.571	9.140	9.674	10.179	14.275
0.200	0.600	4.675	5.668	6.501	7.234	7.898	8.510	9.080	9.616	10.124	14.232
0.200	1.000	4.616	5.604	6.438	7.175	7.842	8.456	9.028	9.566	10.076	14.197
0.200	2.000	4.552	5.545	6.384	7.125	7.795	8.413	8.987	9.527	10.038	14.166
0.400	0.200	4.869	6.039	6.957	7.724	8.397	9.007	9.571	10.098	10.596	14.622
0.400	0.400	4.920	5.938	6.767	7.493	8.148	8.750	9.312	9.839	10.339	14.400
0.400	0.600	4.848	5.830	6.652	7.377	8.034	8.639	9.203	9.734	10.237	14.316
0.400	1.000	4.739	5.714	6.539	7.268	7.930	8.539	9.107	9.641	10.147	14.235
0.400	2.000	4.624	5.607	6.440	7.175	7.841	8.454	9.024	9.559	10.066	14.170
0.500	0.200	4.965	6.167	7.094	7.860	8.531	9.139	9.700	10.225	10.721	14.728
0.500	0.400	5.016	6.033	6.859	7.581	8.232	8.832	9.390	9.916	10.414	14.458
0.500	0.600	4.926	5.903	6.721	7.443	8.096	8.699	9.261	9.790	10.291	14.351
0.500	1.000	4.794	5.765	6.586	7.313	7.971	8.578	9.144	9.676	10.180	14.243
0.500	2.000	4.658	5.636	6.466	7.198	7.860	8.468	9.035	9.567	10.072	14.171
0.600	0.200	5.060	6.290	7.223	7.989	8.657	9.262	9.821	10.344	10.838	14.829
0.600	0.400	5.107	6.122	6.944	7.663	8.312	8.909	9.466	9.990	10.486	14.513
0.600	0.600	4.998	5.972	6.787	7.505	8.156	8.757	9.317	9.843	10.342	14.377
0.600	1.000	4.847	5.814	6.632	7.355	8.011	8.616	9.179	9.708	10.208	14.248
0.600	2.000	4.689	5.665	6.490	7.218	7.875	8.479	9.042	9.572	10.075	14.171
0.650	0.200	5.107	6.350	7.285	8.050	8.717	9.321	9.879	10.401	10.894	14.878
0.650	0.400	5.151	6.164	6.985	7.703	8.351	8.947	9.502	10.025	10.520	14.539
0.650	0.600	5.033	6.005	6.818	7.536	8.185	8.785	9.344	9.869	10.367	14.387
0.650	1.000	4.872	5.837	6.654	7.376	8.030	8.634	9.195	9.722	10.219	14.250
0.650	2.000	4.705	5.678	6.502	7.226	7.880	8.482	9.044	9.574	10.076	14.171
0.700	0.200	5.153	6.408	7.345	8.109	8.775	9.378	9.935	10.456	10.949	14.926
0.700	0.400	5.194	6.205	7.025	7.742	8.388	8.983	9.538	10.060	10.554	14.562
0.700	0.600	5.066	6.037	6.849	7.565	8.214	8.812	9.370	9.895	10.392	14.395
0.700	1.000	4.896	5.860	6.675	7.396	8.049	8.651	9.210	9.734	10.230	14.251
0.700	2.000	4.720	5.692	6.512	7.233	7.885	8.485	9.046	9.575	10.077	14.172
0.800	0.200	5.245	6.521	7.460	8.223	8.887	9.488	10.044	10.563	11.054	15.019
0.800	0.400	5.275	6.284	7.102	7.816	8.461	9.054	9.607	10.128	10.621	14.603
0.800	0.600	5.131	6.098	6.908	7.622	8.269	8.865	9.421	9.944	10.438	14.408
0.800	1.000	4.943	5.904	6.717	7.435	8.085	8.682	9.236	9.755	10.246	14.253
0.800	2.000	4.749	5.717	6.531	7.245	7.892	8.489	9.049	9.577	10.078	14.172
0.900	0.200	5.334	6.629	7.569	8.330	8.993	9.592	10.146	10.665	11.154	15.109
0.900	0.400	5.352	6.359	7.174	7.887	8.531	9.122	9.674	10.192	10.684	14.637
0.900	0.600	5.192	6.157	6.965	7.677	8.322	8.916	9.470	9.989	10.480	14.417
0.900	1.000	4.988	5.947	6.757	7.472	8.118	8.709	9.257	9.771	10.258	14.254
0.900	2.000	4.778	5.740	6.546	7.254	7.897	8.492	9.051	9.578	10.079	14.172
1.000	0.200	5.422	6.733	7.674	8.432	9.093	9.691	10.244	10.762	11.251	15.195
1.000	0.400	5.426	6.430	7.244	7.955	8.597	9.188	9.738	10.255	10.744	14.663
1.000	0.600	5.250	6.213	7.020	7.730	8.373	8.965	9.516	10.031	10.517	14.424
1.000	1.000	5.031	5.988	6.795	7.507	8.146	8.731	9.274	9.784	10.267	14.255
1.000	2.000	4.805	5.760	6.558	7.260	7.900	8.495	9.052	9.579	10.080	14.172

For a fully baffled, agitated vessel, the power number is independent of the Reynolds number in the turbulent region (Bates et al., 1963). Thus,

$$P = K_T d_I^5 N^3 \rho_M \tag{28}$$

The energy dissipation rate per unit mass of liquid in turbulent flow ϵ can therefore be obtained by dividing Eq. 28 by $(\pi/4)\,T^2 H \rho_M$:

$$\epsilon = \frac{4K_T}{\pi}\,\frac{d_I^5 N^3}{T^2 H} \tag{29}$$

By combining Eqs. 26, 27, and 29, and rearranging into dimensionless groups,

$$\frac{k}{\sqrt{N\mathscr{D}}} = C_o\left(\frac{d_I}{T}\right)^{0.5}\left(\frac{d_I}{H}\right)^{0.25}\left(\frac{d_I^2 N\rho}{\mu}\right)^{0.25} \tag{30}$$

For the continuous phase and the usual case of $T = H$,

$$\frac{k_c}{\sqrt{N\mathscr{D}}} = C_o\left(\frac{d_I}{T}\right)^{0.75}\left(\frac{d_I^2 N\rho_c}{\mu_c}\right)^{0.25} \tag{31}$$

Variation of the dispersed phase fraction, ϕ, may modify this relationship in some way yet to be determined.

EXPERIMENTAL APPARATUS AND PROCEDURE

Choice of Materials

Solvents. Water and mixtures of water and sugar (20% and 30% of sugar by weight) were selected for the continuous phase. Two cSt Dow Corning 200 Fluid, ethyl acetate, and benzaldehyde were used in turn for the dispersed phase.

Solute. To study continuous-phase-controlled mass transfer, it is necessary to keep most of the resistance to transfer inside the continuous phase. This requires that the distribution ratio for a solute between the continuous and dispersed phase is large and in favor of the dispersed phase. The solute should also have low rates of transfer so that the concentration changes with time could be measured accurately in batch operation.

Heptanoic acid was chosen for a solute for all five systems. It was highly soluble in all three organic solvents, but its solubility in water is only 0.25 parts per 100 parts of water at 15°C. Octanoic acid was also a good solute, as recommended by Rushton et al. (1964), in view of its distribution ratio and rate of transfer, but it made the mixture of two phases too cloudy to measure droplet size.

The five systems chosen are listed in Table 2. Each dispersed and continuous phase was mutually saturated before mixing runs began. All chemicals used were highly purified re-agent grade.

TABLE 2. FIVE SYSTEMS STUDIED.

System	Dispersed Phase	Continuous Phase	Solute
1	2 cSt Dow Corning⁺ 200 Fluid	Water*	Heptanoic acid
2	2 cSt Dow Corning⁺ 200 Fluid	Water* + 20% sucrose×	Heptanoic acid
3	2 cSt Dow Corning⁺ 200 Fluid	Water* + 30% sucrose×	Heptanoic acid
4	Ethyl Acetate	Water*	Heptanoic acid
5	Benzaldehyde	Water*	Heptanoic acid

* Double-distilled water
⁺ Clear dimethyl siloxane
× Colonial pure cane sugar

TABLE 3. PHYSICAL AND TRANSPORT PROPERTIES AT 23°C

System	σ N/m	ρ_c kg/m³	ρ_d kg/m³	μ_c N · s/m²	μ_d N · s/m²	$\mathscr{D}_c \times 10^{10}$ m²/s
1	0.039	1000	873	0.0010	0.0019	6.01
2	0.032	1087	873	0.0018	0.0019	5.66
3	0.033	1131	873	0.0029	0.0019	4.02
4	0.006	1000	894	0.0010	0.00046	6.01
5	0.015	1000	1041	0.0010	0.0014	6.01

TABLE 4. APPARATUS DIMENSIONS.

	Size A, m	Size B, m
Internal diameter of vessel, T	0.210	0.246
Height of vessel	0.250	0.310
Liquid height in vessel, H	0.210	0.246
Diameter of shaft	0.014	0.014
Baffle length	0.230	0.290
Baffle width	0.019	0.019
Baffle thickness	0.0031	0.0031
Length of baffle immersed in the liquid from air-liquid interface	0.193	0.229

Measurement of Physical and Transport Properties

Interfacial tension was obtained using the Fisher Surface Tensiometer Model 20. The force necessary to pull a platinum-iridium du Nuoy ring through the liquid-liquid interface was measured. Viscosity was determined by using the U. L. adapter of the Brookfield Synchro-Lectric Viscometer manufactured by Brookfield Engineering Laboratories, Inc. Density was measured with the G and A Chain Gravitometer manufactured by Eimer and Amend.

Values of the molecular diffusivity were calculated using existing correlations. The diffusivity of heptanoic acid in pure distilled water was computed from the Bidstrup and Geankoplis (1963) modified correlation of Wilke and Chang (1955) for carboxylic acids:

$$\mathscr{D}_{AB} = \frac{6.6 \times 10^{-8}(\xi M_B)^{1/2} T'}{\mu_{AB} V_{bA}^{0.6}} \tag{32}$$

The diffusivity of heptanoic acid in sucrose solution was calculated by Scheibel's (1954) correlation.

$$\mathscr{D}_{AB} = 8.2 \times 10^{-8}\left[1 + \left(\frac{3V_{bB}}{V_{bA}}\right)^{2/3}\right]\left[\frac{T'}{\mu_{AB} V_{bA}^{1/3}}\right] \tag{33}$$

The physical and transport properties thus obtained are shown in Table 3.

Description of Apparatus

Figure 2 shows the experimental setup. The mixing vessels are two sizes of flat bottomed, cylindrical glass jars which are fitted with four equally spaced, radial, vertical wall baffles, and whose dimensions are listed in Table 4.

A Model ELB experimental agitator kit manufactured by Bench Scale Equipment Co. was used for mixing the liquids. It was equipped with a ¼ hp drive motor, and provided a continuously variable output speed of 0 to 18 rps. The speed-control dial was calibrated directly in rps using a tachometer.

The impellers studied were stainless steel six-flat-blade turbines, since this type showed the best dispersion performance as reported by Skelland and Lee (1978). The diameters of the impellers were 0.078 and 0.106 m, and they were centrally located.

The total interfacial area during mixing was determined from photographs of the dispersions taken through the plane glass water pocket (E of Figure 2). This was attached to the vessel wall and filled with water to eliminate optical distortion. Illumination was provided by a Hedler "Jet-Lux 1250" tungsten-halogen lamp mounted beside the vessel. The camera used was a Nikon F-2 with 55 mm f/3.5 Micro-Nikkor-P lens and MD-2 motor drive. The M2 Ring was inserted between the camera and the Micro-Nikkor-P for the picture with reproduction ratio 1:1 (actual size). Kodak Tri-X Pan film with ASA 400 was used with a shutter speed of 1/1000 ~ 1/2000 second and aperture setting of f/3.5 ~ f/8.0.

The change of solute concentration was measured by monitoring electrical conductivity as recommended by Rushton et al. (1964). The method of sampling the continuous phase through a tubular, fritted glass filter, followed by titration, was tried and found to be unsuitable for batch operation, because of rapidly changing solute concentrations. However, the latter procedure was employed successfully for continuous operation by Schindler and Treybal (1968).

A conductivity cell (D of Figure 2) was made by sealing two platinum wires in an 8-mm pyrex glass tube 0.30 m in length. The exposed portions of the platinum wires were 9.7 mm long and separated by a distance of 1.5 mm, and their ends were joined with a bead of soft glass. The other ends of the electrodes in the glass tube were welded onto copper wires for connection to a "Leeds and Northrup" conductivity monitor. The output of this monitor was recorded simultaneously by an "Electronik 19" recorder manufactured by Honeywell.

The calibration curve giving the conductivity vs. solute concentration was made as follows. First, the relation between the conductivity and solute concentration was obtained without the organic phase. This was achieved by measuring the conductivities of progressively diluted aqueous solutions. Then the effect of the presence of the dispersed organic phase was found in solutions of known concentration. This was done by measuring the conductivities when known fractions of the organic phase were present in uniform dispersion. In this way calibration curves were made for each system studied. These calibrations were found to be independent of the speed and size of the impeller, though the speed should exceed the minimum needed to ensure uniform dispersion.

Caution was needed when obtaining the calibration curves of systems 4 and 5, because ethyl acetate is easily hydrolyzed and benzaldehyde is oxidized in water, to produce weak acid, which changes the conductivity reading as time elapses. Every care was taken to provide the same conditions for the calibration and the actual experimental runs.

The power consumption was measured by the dynamometer assembly, which included a precision force gauge attached to the mounting stand with two positions on the moment arm to increase reading accuracy in the low torque range. The measurements were found to be in reasonable agreement with predictions from the relationships given by Bates et al. (1963) for single phase systems.

Experimental Procedure

The continuous and dispersed phases of each system were prepared separately by presaturating each liquid with the other. A certain amount of heptanoic acid was dissolved in the material for the dispersed phase.

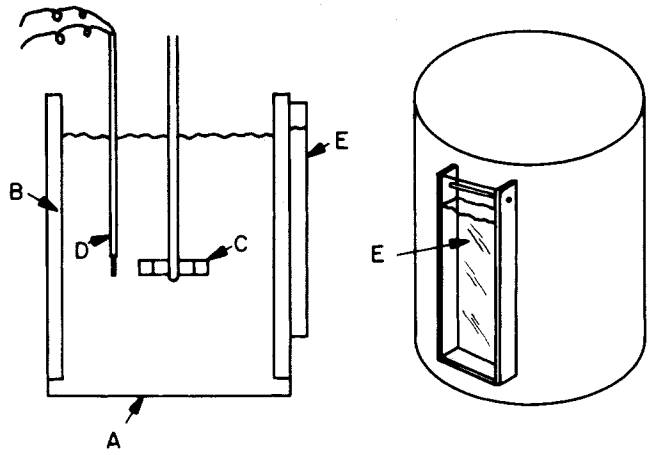

A : Cylindrical Glass Vessel

B : Baffle

C : Six-Flat-Blade Turbine

D : Conductivity Cell

E : Water Pocket

Figure 2. Diagram of apparatus.

The continuous phase was placed in the tank and the mixer was started. The impeller speed, N, was always above the minimum impeller speed for 98% gross uniformity (Skelland and Lee, 1978). The conductivity cell was placed in the impeller stream, and the conductivity monitor and recorder were turned on. The prepared solution of dispersed phase was poured rapidly from a beaker into the center of the vessel (i.e., near the impeller shaft). The conductivity was measured and recorded from the moment the dispersed phase was added until no further increase was observed. It took 4 to 10 seconds to obtain total dispersion of the organic phase throughout the vessel, depending on the impeller speed, although more time was needed for the drops to reach equilibrium size.

About ten photographs (reproduction ratio 1:1) were taken at intervals of 2-4 s during each run. The lamp illuminating the vessel was turned on only when a picture was taken, to prevent raising the temperature of the liquids during the experiment. All runs were performed at a temperature of 23 ± 1°C.

After each run, the apparatus was rinsed with double-distilled water. When every run of a particular system had been completed, the apparatus was taken apart, washed with detergent, and rinsed with hot water and double-distilled water.

All liquids were used only once, except for the Dow Corning 200 Fluid, which was chemically and physically stable. Since the solute was transferred from the dispersed phase into the aqueous phase, the oil was readily reusable by adding more solute. However, due to imperfect separation of the oil from the other liquid, new oil was added for each new run.

The photographic film was developed and the negatives projected on graph paper to estimate the drop-size spectrum by counting about 100 drops. The Sauter-mean diameter was then calculated as follows,

$$d_{32} = \frac{\dfrac{\sum n_i d_{pi}^3}{\sum n_i d_{pi}^2}}{\text{magnification ratio}} \tag{34}$$

This method was useful only for small volume fractions of the dispersed phase; ϕ was never greater than 0.09 in this study.

DISCUSSION OF EXPERIMENTAL RESULTS

Since a solute was chosen so that its equilibrium distribution strongly favored the dispersed phase, the overall mass transfer coefficient for the continuous phase (K_c) was nearly equal to the individual coefficient for the same phase (k_c). Accordingly, from a material balance,

$$V_c d\rho_A = k_c A(\rho_A^* - \rho_A)dt \tag{35}$$

integrating

$$ln\frac{\rho_A^* - \rho_A}{\rho_A^* - \rho_{A1}} = -\frac{k_c A}{V_c}(t - t_1) \tag{36}$$

which shows that a plot of $ln[(\rho_A^* - \rho_A)/(\rho_A^* - \rho_{A1})]$ vs. $t - t_1$ gives a straight line whose slope is equal to $-k_c A/V_c$.

In Eq. 36, t_1 is the time at which the start-up disturbance has ceased; it ranged from 4 to 10 s, depending on the degree of turbulence in the mixing vessel. Consequently, $k_c A$ has been obtained by reading the slope of the plot of $ln[(\rho_A^* - \rho_A)/(\rho_A^* - \rho_{A1})]$ vs. $t - t_1$ as follows:

$$k_c A = -(\text{slope})V_c \tag{37}$$

Figure 3 shows a typical plot of $ln[(\rho_A^* - \rho_A)/(\rho_A^* - \rho_{A1})]$ and $ln\, d_{32}$ vs. $t - t_1$. The Sauter-mean diameters d_{32} were obtained from the pictures taken through the upper half of the water pocket throughout this study, since three pictures taken through the upper half, middle, and lower half of the water pocket showed no significant differences beyond the errors caused by reading the films. The values of d_{32} decreased with time and reached the equilibrium size after one to five minutes. The Sauter-mean diameter, when about 50% of the possible mass transfer had occurred, $\overline{d_{32}}$, [i.e., when $(\rho_A^* - \rho_A)/(\rho_A^* - \rho_{A1}) \doteq 0.5$] was chosen and measured for the calculation of the interfacial area, A. This is calculated from $\overline{d_{32}}$ as

$$A = a \cdot V = \frac{6\phi}{\overline{d_{32}}} \cdot V \tag{38}$$

The liquid height, H, was always equal to the tank diameter, T. The reproducibility of the experimental k_c and d_{32} values was usually within 10%. The range of the volume fraction of the dispersed phase ϕ studied was 0.03 to 0.09. For $\phi > 0.09$, it was difficult to take a clear picture of the droplets, because the liquid mixture became cloudy.

Three values of N were used for each impeller and vessel geometry; the overall range was 3 to 8 rps. The lowest N was above the minimum impeller speed for uniform dispersion as defined by Skelland and Lee (1978). N could not be increased to very high values, because the dispersion started emulsifying, making clear pictures difficult to obtain.

Generalized Correlation for k_c

A generalized correlation for k_c was attempted as follows. First, the approximate exponential dependencies of k_c on some independent variables, ϕ, N, d_I, T, μ_c, and ρ_c were obtained by drawing log-log plots for each independent quantity as the only variable (Lee, 1978). Physical properties were varied by using different systems, so that diffusivities, viscosities, densities, and interfacial tension varied simultaneously. It was therefore not

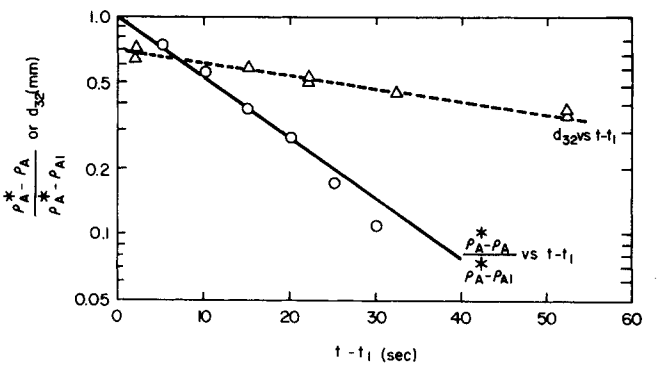

Figure 3. Change of $(\rho_A^* - \rho_A)/(\rho_A^* - \rho_{A1})$ and d_{32} with $t - t_1$ for Run No. 4.

generally possible to establish exponents on these quantities by the same graphical technique. An exception occurred in that a rough estimate of the exponent on ρ_c/μ_c was obtained from the runs on water and the 20% and 30% sugar solutions.

The results of this preliminary graphical treatment are as follows, after incorporating $\mathscr{D}^{0.5}$, as indicated by the theory of periodically varying rate of surface renewal. (The inclusion of $\mathscr{D}^{0.5}$ is considered further below.)

$$k_{c2} \propto \phi^{-0.5} N^{1.7} d_I^{2.95} T^{-0.9} \left(\frac{\rho_c}{\mu_c}\right)^{1.4} \mathscr{D}^{0.5} \tag{39}$$

Next, the SAS (Statistical Analysis System), GLM computer program was used to get the best least-squares correlation for various models that were chosen with the guidance of the periodically varying rate of surface renewal theory and the correlation based on the penetration theory with Kolmogoroff's time scale, as derived earlier.

The selected correlation is

$$\frac{k_c}{\sqrt{N\mathscr{D}}} = 2.932(10^{-7})\phi^{-0.508}\left(\frac{d_I}{T}\right)^{0.548}(N_{Re})^{1.371} \tag{40}$$

for $T = H$. This expression contains the least number of dimensionless groups, and has a correlation coefficient R of 0.8892, an average absolute deviation* of 23.8%, and a certainty of correlation that is better than 99.9%. [In general, for more than 102 data points, R>0.3211 shows the certainty of correlation to be better than 99.9% (Fisher and Yates, 1963)]. Expansion of Eq. 40 gives

$$k_c = 2.932(10^{-7})\phi^{-0.508} N^{1.871} d_I^{3.29} T^{-0.548} \rho_c^{1.371} \mu_c^{-1.371} \mathscr{D}^{0.5} \tag{41}$$

The exponential dependencies of these variables are roughly consistent with those in Eq. 39, obtained by log-log plots. Figure 4 is a plot of the experimental values vs. those predicted by Eq. 40.

Figure 4 shows that the points for the low interfacial tension systems 4 and 5 are not evenly distributed around the diagonal, but deviate systematically to the right of the line. A similar but smaller deviation in the other direction is noted for the high interfacial tension systems 1, 2, and 3. Separate correlations for high and low interfacial tension systems were therefore attempted.

The selected correlation for the high interfacial tension systems with $T = H$ is as follows, with a correlation coefficient of 0.9302 and an average absolute deviation of 20.0%.

$$\frac{k_c}{\sqrt{N\mathscr{D}}} = 2.344(10^{-7})\phi^{-0.529}\left(\frac{d_I}{T}\right)^{0.701}(N_{Re})^{1.394} \tag{42}$$

For the low interfacial tension systems only 12 runs were made, covering but a small range of N_{Re} and without variation of d_I/T. Thus the exponential dependencies of N_{Re} and d_I/T for these systems were assumed to be the same as those of Eq. 40, and the best least squares correlation was obtained tentatively as follows, where $T = H$:

$$\frac{k_c}{\sqrt{N\mathscr{D}}} = 1.864(10^{-6})\phi^{-0.287}\left(\frac{d_I}{T}\right)^{0.548}(N_{Re})^{1.371}(N_{We})^{-0.095} \tag{43}$$

The correlation coefficient and the absolute average deviation were 0.8508 and 7.3%, respectively.

Effect of Diffusivity

The influence of diffusivity on the mass transfer coefficient is central to the question of which transport mechanism is prevailing in the situation at hand. Thus, in the expression

$$k_c \propto \mathscr{D}^n$$

the exponent n has a value of unity according to the film theory,

*Absolute deviation is defined as |(Predicted value-Observed Value)/Observed value| throughout this study.

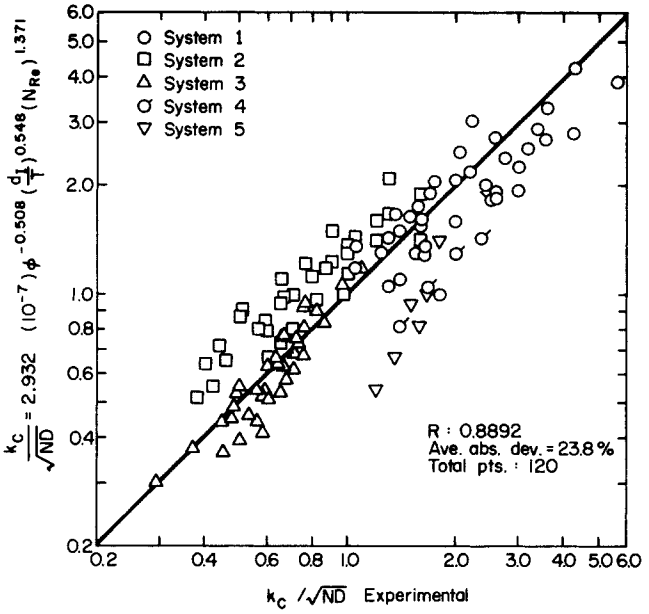

Figure 4. Predicted $k_c/\sqrt{N\mathscr{D}}$ from Eq. 40 vs. experimental $k_c/\sqrt{N\mathscr{D}}$.

whereas values between ½ and one are consistent with the film-penetration theory of Toor and Marchello (1958) and Dobbins (1956, 1964). Other theoretical mechanisms, including some that permit n to approach zero, are reviewed by Kozinski and King (1966). When the interface is mobile an n of ½ is indicated by the eddy cell model (Lamont and Scott, 1970), by boundary layer theory (Calderbank, 1967), by the large-eddy model (Fortesque and Pearson, 1967), by turbulent boundary layer and slip velocity theory (Keey and Glen, 1969), and by potential flow theory (Calderbank, 1967). An n value of ½ also follows from our theory of periodically varying rate of surface renewal. On the other hand, for immobile interfaces, n equals ⅔ according to the eddy cell model (Lamont and Scott, 1970), to boundary layer theory (Calderbank, 1967), and to slip velocity theory for "large" particles (Harriott, 1962).

When attention is confined to mass transfer in two-phase suspensions in agitated vessels, the experimental findings are conflicting and often at variance with theory. Thus it was contended that n equals zero by Barker and Treybal (1960). This was reiterated in two subsequent publications by Treybal (1961, 1963, p. 417).

For mass transfer from solid particles freely suspended in agitated liquids (i.e., immobile interfaces), an n of ⅔ was obtained by Calderbank and Moo-Young (1961). This contrasts with n values of ½ found by Hixson and Baum (1941), Bieber (1962), Barker and Treybal (1960), and Sykes and Gomezplata (1967). In the work of Barker and Treybal, a 170-fold range of $\mathscr{D}$ was used to establish a value of ½ for n by graphical means. Sykes and Gomezplata specifically showed that an n of ½ satisfactorily represented their results, whereas ⅔ did not. They observed that "the over correction for the effect of system Schmidt number (and therefore of $\mathscr{D}$) . . . by the fixed particle correlations (i.e., by use of n = ⅔) has been noted by Miller (1964)."

Both Harriott (1962) and Calderbank (1967) state that small drops and bubbles behave as rigid spheres when suspended in agitated liquids. The resulting immobile interface would suggest that n equals ⅔, according to some of the above theories. Thus Calderbank's (1967) correlation of measurements for small bubbles in aqueous electrolytes uses n = ⅔. Both Treybal (1963, p. 416) and Glen (1965), on the other hand, say that the surface of such liquid drops is mobile. This is consistent with Prasher and Wills' (1973) use of n = ½ to correlate mass transfer from gas bubbles in agitated liquids.

Whether the drops of disperse phase in the present work possessed mobile or immobile interfaces is unknown, although

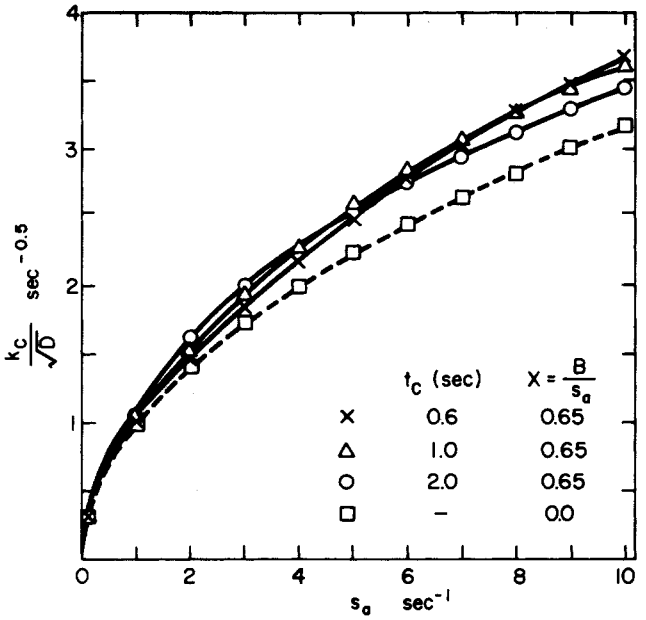

Figure 5. s_a vs. $k_c/\sqrt{\mathcal{D}}$ for $x = 0.65$ for low range of s_a.

mobility may have been present at least in the low-interfacial-tension systems 4 and 5. In any event, definitive information on n is not forthcoming from the present study, because $\mathcal{D}$ varied only 1.5-fold. Thus, in using $\mathcal{D}$ to the one-half power in Eqs. 40-43, we recognize that the real situation may be

$$k_c \propto \mathcal{D}^{0.5}\mathcal{D}^{n-0.5}$$

where any remaining dependence on $\mathcal{D}$(as $\mathcal{D}^{n-0.5}$) has been incorporated in the numerical constant on the right side of each equation. In this regard, if n should really be, say, ⅔, then the term $\mathcal{D}^{n-0.5}$ varied in our runs by less than ±3.4% about its mid-value because of our small variation in $\mathcal{D}$.

Our approach here, then, is analogous to that of Humphrey and Van Ness (1957) and of Miller (1971), who arbitrarily assigned values of ½ and ⅔, respectively, to n, even though they each studied only one system of solid particles dissolving in an agitated liquid. Clearly $\mathcal{D}$ and N_{Sc} were not variables in their work.

It is useful to compare our results with those of Keey and Glen (1969) and Schindler and Treybal (1968).

Keey and Glen worked with a single ternary system. The values of k_c predicted by their correlation were much lower than our observed values, with an average absolute deviation of 58.2%. This discrepancy possibly arises because the interfacial tension for their correlation (0.0504 N/m) is substantially higher than the upper limit for ours; also their correlation is for continuous—not batch—operation and does not include the effect of ϕ, the fraction of the dispersed phase present.

Schindler and Treybal, on the other hand, worked with a binary system of low interfacial tension. In comparing their correlation (Eq. 2) with our data, k_s was calculated by the procedure described in Harriott's paper (1962), as recommended by Schindler and Treybal. The second term, 3.94 $(\mathcal{D}_A/\theta_c)^{0.5}$, was approximated from their conclusion that its typical contributions to k_c were: zero ($\phi = 0.01$, $N_{Re} = 31{,}000$ and $\phi = 0.0240$, $N_{Re} = 20{,}750$), 17% ($\phi = 0.015$, $N_{Re} = 30{,}000$), 35% ($\phi = 0.0374$, $N_{Re} = 20{,}750$), and 53% ($\phi = 0.0509$, $N_{Re} = 46{,}250$). Some of the values predicted by the above method were close to our observed values, but the points were scattered widely, with an average absolute deviation of 34.1%. This could be partly due to their anomalous increase of k_c with increasing ϕ, as noted in their paper.

Generalized Correlation for s_a

Attempts were made to obtain a generalized correlation of the average rate of surface renewal in the continuous phase near each droplet, s_a, from the observations of mass transfer rate.

First, s_a was compared with the rate of surface renewal s_D, defined by Danckwerts, which can be calculated from his result as

$$s_D = k^2/\mathcal{D} \tag{44}$$

s_a can be obtained from each experimental value of k_c by using Eq. 20 and Table 1. The values of $x = B/s_a$ for all 120 runs varied from 0.56 to 0.70. s_a obtained by assuming $x = 0.65$ throughout gave correct values to two significant figures. The values of s_a were therefore interpolated from Figures 5 and 6 which are the plots of Table 1 for $x = 0.65$. The broken lines in Figures 5 and 6 represent s_D from Danckwerts' surface renewal theory (Eq. 44).

The average deviation of s_D from s_a, expressed as $(s_D - s_a)/s_a$, was calculated to be + 0.193. In other words, s_D is higher than s_a by an average of 19.3%, which seems to be a significant difference.

A general correlation for s_a was obtained by a procedure similar to that used for the k_c correlation for $T = H$ as

$$\sqrt{\frac{s_a}{N}} = 4.453(10^{-7})\phi^{-0.502}\left(\frac{d_I}{T}\right)^{0.592}(N_{Re})^{1.328} \tag{45}$$

The correlation coefficient R and the average absolute deviation were 0.8805 and 24.7%, respectively. Figure 7 shows predicted $\sqrt{s_a/N}$ vs. experimental $\sqrt{s_a/N}$. The certainty of correlation is better than 99.9% (Fisher and Yates, 1963).

As a result, the mass transfer coefficient for the continuous phase, k_c, could alternatively be obtained from physical properties of the liquids and the geometry of the apparatus by the following procedure:

1) Calculate s_a from Eq. 45,
2) Compute t_c from the correlation by Holmes et al. (1964), given in Eq. 21.
3) Evaluate x from Eq. 22.
4) Obtain the value of k_c by interpolating from Table 1 for the known values of s_a, t_c and x.

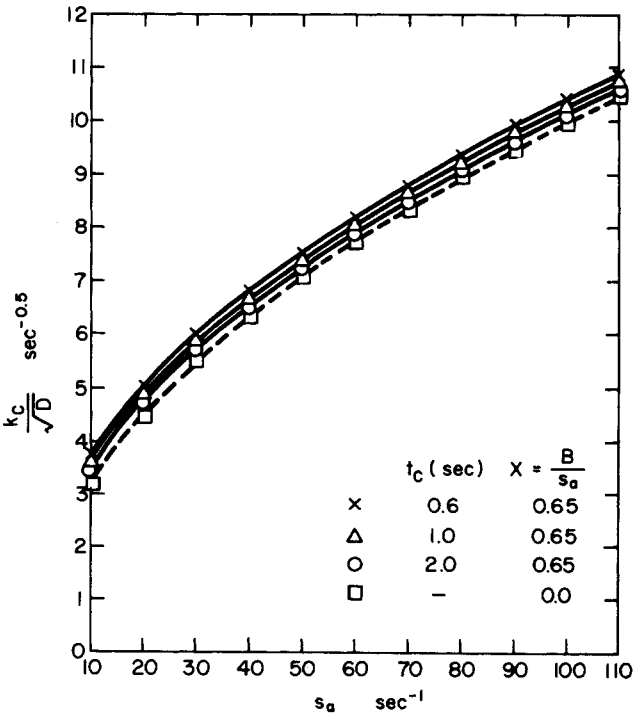

Figure 6. s_a vs. $k_c/\sqrt{\mathcal{D}}$ for $x = 0.65$ for high range of s_a.

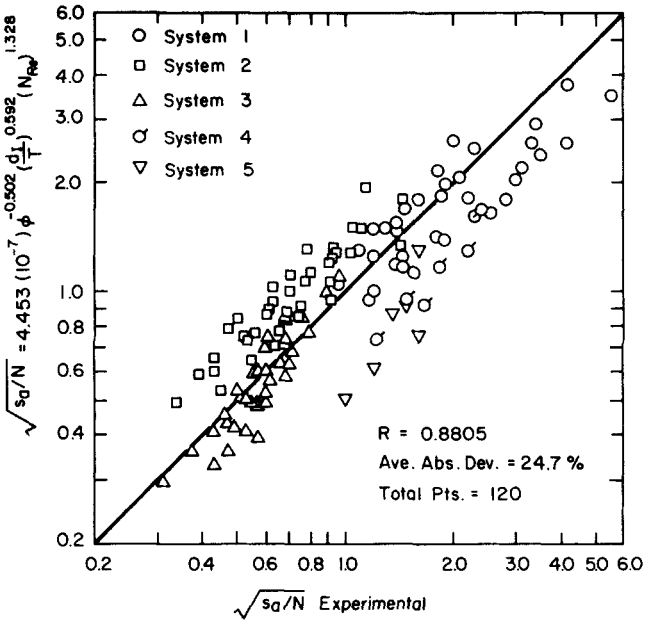

Figure 7. Predicted vs. experimental $\sqrt{s_a/N}$ values.

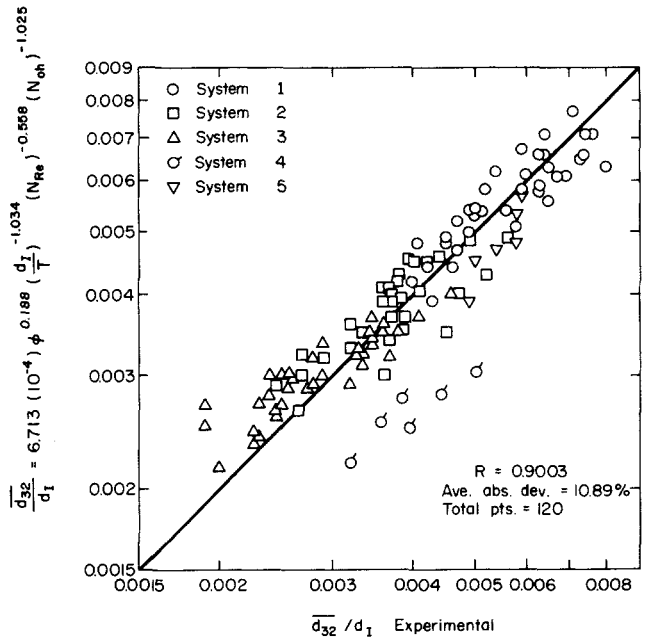

Figure 8. Predicted vs. experimental $\overline{d_{32}}/d_1$ values.

However, since Eq. 40 is already available for predicting k_c, of more interest is the possible eventual use of the s and s_a correlations in predicting the effect of a chemical reaction on the rate of mass transfer (Sherwood et al., 1975c; Danckwerts, 1970).

Generalized Correlation for $\overline{d_{32}}$

The Sauter-mean droplet diameter when about 50% of the possible mass transfer had occurred was chosen for correlation as an average value during batch operation. The selected correlation is

$$\frac{\overline{d_{32}}}{d_I} = 6.713(10^{-4})\phi^{0.188}\left(\frac{d_I}{T}\right)^{-1.034}(N_{Re})^{-0.558}(N_{Oh})^{-1.025} \quad (46)$$

The correlation coefficient R and the average absolute deviation were 0.9003 and 10.9%, respectively, and the certainty of correlation is better than 99.9% (Fisher and Yates, 1963). The predicted vs. experimental values of $\overline{d_{32}}/d_I$ are plotted in Figure 8.

A comparison between the observed $\overline{d_{32}}$ and existing correlations, including ours, is shown in part in Figure 9. Eq. 8 is not represented in this Figure, because it is based on only one liquid-liquid system and therefore does not include physical properties as variables. The discrepancies between observed values and those predicted by Thornton (1963), Coulaloglou (1976), Mlynek (1972), and Sprow (1967) are generally large, although Thornton's relation is closer than the others. The deviations may arise because the previous correlations are for steady-state operation without mass transfer, whereas these observed $\overline{d_{32}}$ are measured at the moment when about 50% of the possible mass transfer has occurred. In any event, disagreement among the previous relationships themselves is substantial, as shown by Figure 9.

Optimization Procedure

Increasing impeller speed, N, will increase both the mass transfer coefficient, k, and the interfacial area per unit volume, a. This means that the volume of mixing vessel V needed for a specified transfer rate and stage efficiency will decrease. On the other hand, the power P consumed by the impeller will increase. This shows that an optimum impeller speed exists at which the total annual cost is a minimum, where

$$\text{Total annual cost} = C_T = \text{annual fixed charge on the vessel, } C_F, + \text{annual power cost, } C_P \quad (47)$$

For a specified stage efficiency and fixed flow rate of extract and raffinate phases, the transfer rate of solute A is fixed at q_A kg/s and, assuming a continuous phase-controlled system, as recommended by Skelland (1967):

$$q_A = k_c A \Delta\rho_A = k_c a V \Delta\rho_A,$$

$$V = \frac{q_A}{k_c a \Delta\rho_A} = \frac{\pi T^3}{4} \text{ for } T = H \quad (48)$$

The annual fixed charges on the vessel, C_F, may be written as

$$C_F = C_1 V^{0.6} \quad (49)$$

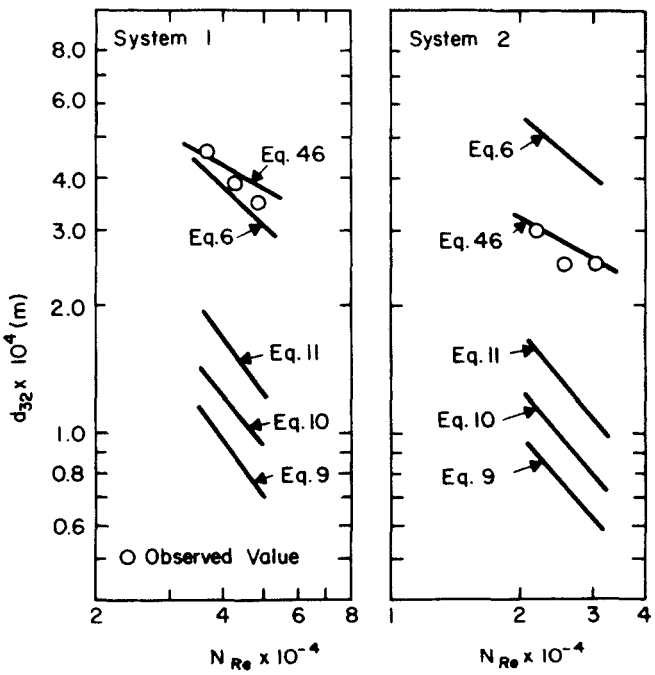

Figure 9. Comparison between some of our experimental Sauter-mean drop diameters and existing correlations.

Fixed: $d_I = 0.078$, $T = 0.210$ m, $\phi = 0.03$.

where the "six-tenths rule" has been invoked to relate the vessel cost to its size (Peters, 1958). Eqs. 40 and 46 may be combined to obtain the continuous-phase capacity coefficient $k_c a$ for six-flat-blade turbines, noting that $a = 6\phi/\overline{d_{32}}$,

$$k_c a = 2.621(10^{-3}) \frac{(N\mathscr{D})^{\frac{1}{2}}}{d_I} \phi^{0.304} \left(\frac{d_I}{T}\right)^{1.582} (N_{Re})^{1.929} (N_{Oh})^{1.025} \quad (50)$$

Then, for a given ϕ and fixed fluid properties

$$k_c a = C_2 N^{2.429} d_I^{2.3455} \lambda^{1.582} \quad (51)$$

where $\lambda = d_I/T$.

For turbulent agitation of Newtonian fluids in fully baffled vessels the power number, $P/d_I^5 N^3 \rho_M$, is independent of Reynolds number (Skelland, 1967). Bates et al. (1963) reported that an effect of the d_I/T ratio on power consumption exists with six-flat-blade turbines, but it is negligible for baffle widths of $T/8$ to $T/14$ when d_I/T is between 0.25 and 0.5. Four $T/12$ baffles are commonly employed in industry as a standard (Bates et al., 1963). Therefore, for fixed fluid properties and $0.25 \leq d_I/T \leq 0.5$

$$C_p = C_3 P = C_4 N^3 d_I^5 \rho_M = C_5 N^3 d_I^5 \quad (52)$$

Combining Eqs. 47, 48, 49, 51, and 52.

$$C_T = C_1 \left[\frac{q_A}{C_2 \Delta\rho_A}\right]^{0.6} N^{-1.4574} d_I^{-1.4073} \lambda^{-0.9492} + C_5 N^3 d_I^5 \quad (53)$$

From Eq. 48,

$$V = \frac{q_A}{k_c a \Delta\rho_A} = \frac{\pi T^3}{4} = \frac{\pi d_I^3}{4\lambda^3} \quad (54)$$

Substituting Eq. 51 into Eq. 54 and rearranging.

$$d_I = \left(\frac{4 q_A}{\pi C_2 \Delta\rho_A}\right)^{1/5.3455} N^{-0.4544} \lambda^{0.2653} \quad (55)$$

Insertion of Eq. 55 into Eq. 53 gives

$$C_T = C_1 \left(\frac{4}{\pi}\right)^{-0.2633} \left(\frac{q_A}{C_2 \Delta\rho_A}\right)^{0.3367} N^{-0.8179} \lambda^{-1.3226} + C_5 \left(\frac{4}{\pi}\right)^{0.9354} \left(\frac{q_A}{C_2 \Delta\rho_A}\right)^{0.9354} N^{0.728} \lambda^{1.3265} \quad (56)$$

In industry the standard value for $\lambda = d_I/T$ is usually 0.33 (Bates et al., 1963). Therefore, differentiating the above equation with respect to N, equating to zero for minimum total cost, and solving for the optimum impeller speed at a given ratio of impeller-to-tank diameter, λ_1,

$$N_{\text{opt.}} = 0.894 \left(\frac{C_1}{C_5}\right)^{0.6469} \left(\frac{q_A}{C_2 \Delta\rho_A}\right)^{-0.3873} \lambda_1^{-1.7136} \quad (57)$$

The optimum impeller diameter is then obtained by inserting Eq. 57 for N in Eq. 55. The optimum volume of the mixing vessel, $V_{\text{opt.}}$, can also be formulated by combining Eqs. 54, 55, and 57 for $\lambda = \lambda_1$.

$$V_{\text{opt.}} = 1.0479 \left(\frac{C_1}{C_5}\right)^{-0.882} \left(\frac{q_A}{C_2 \Delta\rho_A}\right)^{1.0893} \lambda_1^{0.132} \quad (58)$$

The optimum power consumption is obtained by inserting Eq. 57 with Eq. 55 for $d_{I,\text{opt}}$ into Eq. 52, again for $\lambda = \lambda_1$.

$$P_{\text{opt.}} = 1.1554 \frac{C_5}{C_3} \left(\frac{C_1}{C_5}\right)^{0.4707} \left(\frac{q_A}{C_2 \Delta\rho_A}\right)^{0.6536} \lambda_1^{0.0792} \quad (59)$$

Several values of λ can then be tried, with Eqs. 56 and 57, to obtain the overall minimum total cost. (The constant C_5 will remain unchanged for $0.25 \leq \lambda \leq 0.5$). $N_{\text{opt.}}$ should be above the minimum impeller speed for uniform mixing but low enough to avoid emulsification. In short, the feasibility of using the optimum conditions should be assessed in each particular application.

Scale-Up

In some cases, instead of optimizing one's design for minimum total cost, it may be necessary to ensure the same mass transfer rate per unit volume on two different scales of operation.

To obtain equal capacity coefficients in two geometrically similar vessels of different size, when $\phi_1 = \phi_2$ and the relevant physical properties have respectively the same values on the two scales, equating the right-hand side of Eq. 50 for systems 1 and 2 leads to

$$\frac{N_1}{N_2} = \left(\frac{T_1}{T_2}\right)^{0.651} \left(\frac{d_{I_2}}{d_{I_1}}\right)^{1.358} \quad (60)$$

This is the ratio of N's between the model and the scaled-up equipment. Since the flow is turbulent, from Eq. 52

$$\frac{P_1}{P_2} = \left(\frac{d_{I_1}}{d_{I_2}}\right)^5 \left(\frac{N_1}{N_2}\right)^3 = \left(\frac{T_1}{T_2}\right)^{1.953} \left(\frac{d_{I_1}}{D_{I_2}}\right)^{0.926} \quad (61)$$

The ratio of the power input per unit volume in the two vessels is then

$$\frac{P_1/Vol_1}{P_2/Vol_2} = \frac{P_1}{P_2} \left(\frac{T_2}{T_1}\right)^3 = \left(\frac{T_2}{T_1}\right)^{1.047} \left(\frac{d_{I_1}}{d_{I_2}}\right)^{0.926} \quad (62)$$

Eq. 62 shows that the power input per unit volume to make $(k_c a)_1 = (k_c a)_2$ decreases with increasing T and decreasing d_I for the range of d_I/T studied.

ACKNOWLEDGMENT

T. J. Suffridge assisted with the integration of Eq. 19. This work was partially supported by the National Science Foundation Grants ENG 74-17286 and ENG 77-14609.

NOMENCLATURE

A = interfacial area in a two-phase mixture, m^2
a = interfacial area per unit volume in a two-phase mixture, 1/m.
B = amplitude of period defined in Figure 1, 1/s.
C, $C_o - C_5$ = constants
C_T = total annual cost
C_F = annual fixed charge on the vessel
C_P = annual power cost
d_I = impeller diameter, m
$\mathscr{D}$ = diffusivity, m^2/s
d_P = particle diameter, m
d_{32} = Sauter-mean droplet diameter defined by $\frac{\Sigma n_i d_{Pi}^3}{\Sigma n_i d_{Pi}^2}$, m
$\overline{d_{32}}$ = Sauter-mean drop diameter when about 50% of the possible transfer has occurred, i.e., when $(\rho_A^* - \rho_A)/(\rho_A^* - \rho_{A1}) \doteq 0.5$, m
d_{32}^o = Sauter-mean droplet diameter at substantially zero dispersed phase holdup, m
g = acceleration due to gravity, m/s^2
H = height of liquid in the vessel, m
K = overall mass transfer coefficient, m/s
K_T = constant in Eq. 28
k = individual mass transfer coefficient, m/s
k_c = continuous-phase individual mass transfer coefficient, m/s
k_1, k_3 = constants, defined in Eq. 22
k_s = steady-state continuous-phase mass transfer coefficient, m/s
l = eddy size, m
M_B = molecular weight of component B
N = impeller speed, rps
N_{Oh} = Ohnesorge number, defined by $\frac{\mu_c}{\sqrt{\rho_c d_I \sigma}}$

N_{Re} = impeller Reynolds number, defined by $\rho_c N d_I^2/\mu_c$
N_{Sc} = Schmidt number, $\mu_c/\rho_c \mathcal{D}_c$
N_{Sh} = Sherwood number, defined by $k_c d_I/\mathcal{D}$
N_{We} = impeller Weber number, defined by $N^2 d_I^3 \rho_c/\sigma$
n_{Ao} = mass flux of component A at the interface, kg/m^2·s
P = power dissipated by impeller, N·m/s
P_v = power dissipated by impeller per unit volume of vessel, N/m^2·s
q_A = mass transfer rate of solute A, kg/s
R = Correlation Coefficient, dimensionless
R' = outer radius of continuous-phase shell, m
r_p = mean drop radius, m
r = radius, m
s = fractional rate of surface renewal, 1/s
s_a = average fractional rate of surface renewal, 1/s
s_D = fractional rate of surface renewal, defined by Danckwerts as a constant value, 1/s
T = vessel diameter, m
T' = absolute temperature, °K
t = time, s
t_c = circulation time around the vessel, s
t_e = exposure time defined in the penetration theory, s
t_1 = the time at which the start-up disturbance has ceased, s
$\overline{U}$ = time mean velocity of main flow, m/s
u_t = droplet terminal velocity in the continuous-phase, m/s
V = filled volume of vessel, m^3
V_{bA}, V_{bB} = critical volumes of pure liquid components A and B at their normal boiling temperatures, cm^3/gm-mol for Eqs. 32 and 33.
V_c = volume of the continuous-phase, m^3
v = Kolmogoroff's velocity scale, defined by Eq. 24, m/s
x = B/s_a, dimensionless
ϵ = rate of energy dissipation per unit mass of fluid, m^2/s^3
λ = d_I/T, dimensionless
θ_c = time between coalescences, s
μ = viscosity, N·s/m^2
μ_{AB} = viscosity of the solution, N·s/m^2, *cP* for Eqs. 32 and 33.
ν = kinematic viscosity, m^2/s
ξ = an "association" factor for the solvent B, dimensionless
ρ = density, kg/m^3
ρ_A, ρ_A^*, ρ_{A1}, $\rho_{A\infty}$ = mass concentration of component A; interfacial value in the phase under consideration; at t_1; at $t \rightarrow \infty$, kg/m^3
ρ_M = mean density of two-phase mixture, kg/m^3 (Treybal, 1963 p. 415)
$\Delta\rho$ = positive density difference between continuous and disperse phases, kg/m^3
η = Kolmogoroff's length scale, defined by Eq. 23, m
σ = interfacial tension, N/m
τ_k = Kolmogoroff's time scale, defined by Eq. 25, s
ϕ = volume fraction of dispersed phase, dimensionless
$\phi(t)$ = surface age distribution function, 1/s

Subscripts

c = continuous phase
d = dispersed phase

LITERATURE CITED

Banerjee, S., D. Scott, and E. Rhodes, "Mass Transfer to Falling Wavy Liquid Films in Turbulent Flow," *I&EC Fundamentals*, **7**, 22 (1968).
Barker, J. J., and R. E. Treybal, *AIChE J.*, **6**, 289 (1960).
Bates, R. L., P. L. Fondy, and R. R. Corpstein, "An Examination of Some Geometric Parameters of Impeller Power," *I&EC Process Des. Develop.*, **2**, 310 (1963).
Bidstrup, D. E., and C. J. Geankoplis, "Aqueous Molecular Diffusivities of Carboxylic Acids," *J. of Chem. Eng. Data*, **8**, 170 (1963).
Bieber, H., Sc.D. Thesis, Columbia Univ., New York (1962).
Brodkey, R. S., "The Phenomena of Fluid Motions," 291-2, Addison Wesley, MA (1967).
Calderbank, P.H., "Mixing," **II**, V. W. Uhl and J. B. Gray, eds., Academic Press, New York (1967).
Calderbank, P. H., and M. B. Moo-Young, "The Continuous Phase Heat and Mass Transfer Properties of Dispersions," *Chem. Eng. Sci.*, **16**, 39 (1961).
Coulaloglou, C. A., and L. L. Tavlarides, "Drop Size Distributions and Coalescence Frequencies of Liquid-Liquid Dispersions in Flow Vessels," *AIChE J.*, **22**, 289 (1976).
Danckwerts, P. V., "Significance of Liquid-Film Coefficients in Gas Absorption," *Ind. Eng. Chem.*, **43**, 1460 (1951).
Danckwerts, P. V., "Gas-Liquid Reactions," Ch. 5, McGraw-Hill, New York (1970).
Dobbins, W. E., "Biological Treatment of Sewage and Industrial Wastes," Part 2-1, M. L. McCabe and W. W. Eckenfelder, eds., Reinhold, New York (1956).
Dobbins, W. E., Int. Conf. on Water Pollut. Res., Lond., Sept. 1962, Pergamon Press, New York, 61 (1964).
Fisher, R. A. and F. Yates, "Statistical Tables for Biological, Agricultural and Medical Research," 6th ed., Oliver and Boyd, Edinburgh (1963).
Fortesque, G. E. and J. R. A. Pearson, *Chem. Eng. Sci.*, **22**, 1163 (1967).
Glen, J. B., "Mass Transfer in Disperse Systems," Ph.D. Dissertation, University of Canterbury, Christchurch, New Zealand (1965).
Harriott, P., "Mass Transfer to Particles: Part 1. Suspended in Agitated Tanks," *AIChE J.*, **8**, 93 (1962).
Higbie, R., "The Rate of Absorption of a Pure Gas into a Still Liquid During Short Periods of Exposure," *Trans. AIChE*, **31**, 365 (1935).
Hinze, J. O., "Turbulence," 2nd ed., 223, 399, McGraw-Hill, New York (1975).
Hixson, A. W., and S. J. Baum, *Ind. Eng. Chem.*, **33**, 478 (1941).
Holmes, D. B., R. M. Voncken, and J. A. Dekker, "Fluid Flow in Turbine-stirred, Baffled Tanks—I. Circulation Time," *Chem. Eng. Sci.*, **19**, 201 (1964).
Humphrey, D. W. and H. C. Van Ness, *AIChE J.*, **3**, 283-6 (1957).
Keey, R. B., and J. B. Glen, "Area-Free Mass Transfer Coefficients for Liquid Extraction in a Continuously Worked Mixer," *AIChE J.*, **15**, 942 (1969).
Kozinski, A. A., and C. J. King, *AIChE J.*, **12**, 109 (1966).
Lamont, J. C. and D. S. Scott, "An Eddy Cell Model of Mass Transfer into the Surface of a Turbulent Liquid," *AIChE J.*, **16**, 513 (1970).
Lee, J. M., "Mass Transfer and Liquid-Liquid Dispersion in Agitated Vessels," Ph.D. Dissertation, University of Kentucky, Lexington, KY (1978).
McCabe, W. L., and J. C. Smith, "Unit Operations of Chemical Engineering," 3rd ed., 234, McGraw-Hill, New York (1976).
Miller, D. N., *Ind. Eng. Chem.*, **56**, No. 10, 18 (1964).
Miller, D. N., *Ind. Eng. Chem.*, Process Des. and Dev., **10**, 365 (1971).
Mlynek, Y. and W. Resnick, "Drop Sizes in an Agitated Liquid-Liquid System," *AIChE J.*, **18**, 122 (1972).
Nadkarni, V. M. and T. W. F. Russell, "Mass Transfer to Naturally Flowing Streams," *I&EC Process Des. Develop.*, **12**, 414 (1973).
Nagata, S., K. Yamamoto, K. Hashimoto, and Y. Naruse, "Flow Patterns of Liquids in a Cylindrical Mixing Vessel with Baffles," *Mem. Fac. Eng.*, Kyoto Univ., **21**, 260 (1959).
Peters, M. S., "Plant Design and Economics for Chemical Engineers," 93-4, McGraw-Hill, New York (1958).
Prasher, B. D. and G. B. Wills, "Mass Transfer in an Agitated Vessel," *I&EC Process Des. Dev.*, **12**, 351 (1973).
Rushton, J. H., S. Nagata, and T. B. Booney, "Measurement of Mass Transfer Coefficients in Liquid-Liquid Mixing," *AIChE J.*, **10**, 298 (1964).
Scheibel, E. G., *Ind. Eng. Chem.*, **46**, 2007 (1954).
Schindler, H. D., "Area Based Mass Transfer Coefficients in Liquid Extraction," Ph.D. Dissertation, New York Univ., New York (1967).
Schindler, H. D., and R. E. Treybal, "Continuous-Phase Mass-Transfer Coefficients for Liquid Extraction in Agitated Vessels," *AIChE J.*, **14**, 790 (1968).
Sherwood, T. K., R. L. Pigford, and C. R. Wilke, "Mass Transfer," (a) 220-4, (b) 150-9, (c) Ch. 8, McGraw-Hill, New York (1975).
Sideman, S., O. Hortacsu, and J. W. Fulton, "Mass Transfer in Gas-Liquid Contacting Systems," *Ind. Eng. Chem.*, **58** (7), 32 (1966).
Skelland, A. H. P., "Non-Newtonian Flow and Heat Transfer," 325-7, Wiley, New York (1967).
Skelland, A. H. P., "Diffusional Mass Transfer," (a) 56, (b) 94-102, Wiley-Interscience, New York (1974).
Skelland, A. H. P., and J. M. Lee, "Agitator Speeds in Baffled Vessels for Uniform Liquid-Liquid Dispersions," *I&EC Process Des. Dev.*, **17**, 473 (1978).
Sprow, F. B., "Distribution of Drop Sizes Produced in Turbulent Liquid-Liquid Dispersion," *Chem. Eng. Sci.*, **22**, 435 (1967).

Sykes, P., and A. Gomezplata, *Can. J. Chem. Eng.*, **45**, 189 (1967).
Thornton, J. D., and B. A. Bouyatiotis, "Liquid Extraction Operations in Stirred Vessels," *Ind. Chemist*, **39**, 298 (1963).
Toor, H. L., and J. M. Marchello, *AIChE J.*, **4**, 97-101 (1958).
Treybal, R. E., *Ind. Eng. Chem.*, **53**, 597 (1961).
Treybal, R. E., "Liquid Extraction," 2nd ed., 415, McGraw-Hill, New York (1963).
Treybal, R. E., "Mass-Transfer Operations," 2nd ed., (a) 46-55, (b) 411-2, McGraw-Hill, New York (1968).
Uhl, V. W., and J. B. Gray, "Mixing," **2**, 19-21, Academic Press, New York (1966).
Wilke, C. R., and P. Chang, "Correlation of Diffusion Coefficients in Dilute Solution," *AIChE J.*, **1**, 264 (1955).

Manuscript received June 13, 1979; revision received May 5, and accepted May 12, 1980.

Steady-State Multiplicity of a Nonadiabatic Bubble Column with Fast Reactions

A steady-state model is developed for a nonadiabatic bubble column with fast pseudo-*n*th-order reactions. *A priori* bounds are obtained for steady-state temperature and conversion, and analytic necessary and sufficient criteria are derived for the prediction of uniqueness and multiplicity of the steady states as a function of system physico-chemical parameters. For the special case of pseudo-first-order reactions, the occurrence of multiple steady states is shown to be more possible in a bubble column than in a gas-liquid CSTR for equivalent system parameters.

D. T.-J. HUANG
and
ARVIND VARMA
Department of Chemical Engineering
University of Notre Dame
Notre Dame, Indiana 46556

SCOPE

Because of simple construction and excellent temperature control, bubble columns are frequently applied in the process industries. Recently, they are also gaining increasing importance in biotechnology, particularly in fermentations and waste water treatment due to favorable mixing and mass transfer properties combined with low shear stressing of the biological material.

In the operation of gas-liquid CSTRs, the occurrence of multiple steady states has been experimentally observed (Ding et al. 1974) and theoretically explored (Hoffman et al., 1975; Sharma et al., 1976; Raghuram and Shah, 1977; Raghuram et al., 1979; Huang and Varma, 1981). Because a bubble column is quite similar to a CSTR (one with and the other without mechanical stirring), it may be expected that such phenomenon also occurs in bubble columns. However, as far as the authors are aware, no study has been done of the steady-state multiplicity aspects of bubble columns—either experimentally or theoretically.

In this work, a steady-state model is developed for a nonadiabatic bubble column with fast pseudo-*n*th-order reactions and multiplicity analysis (Varma and Aris, 1977) is performed. For the special case of pseudo-first-order reactions, comparisons are also made between bubble columns and CSTRs regarding the relative possibility of the occurrence of multiple steady states.

CONCLUSIONS AND SIGNIFICANCE

Analytic criteria are derived for the prediction of uniqueness and multiplicity of the steady states in a bubble column as a function of system physico-chemical parameters. These criteria along with the model should help provide a rational approach to the design and optimization of bubble columns.

It is found that the region of multiplicity shrinks as the reaction order increases. This feature is the same as that found for single-phase reactors (Tsotsis and Schmitz, 1979; Chang and Calo, 1979).

For the special case of pseudo-first-order reactions, numerical examples applying the data for the chlorination of *n*-decane (Sharma et al., 1976) to the bubble column show that every multiplicity pattern observed in a gas-liquid CSTR is also possible in the bubble column. Moreover, it is found that the possibility of the occurrence of multiple steady states is greater in the bubble column than in the CSTR. It is also shown that information obtained from gas-liquid CSTRs may be helpful in the design and operation of bubble columns.

DEVELOPMENT OF THE MODEL

It was found that for hydrogen-α-methylstyrene system in a bubble column (Sherwood and Farkas, 1966), the liquid phase was well mixed from top to bottom by the bubbling gas flow, although the ratio of height of gas-liquid mixture to column diameter (L/D) was 12 to 35, and the gas phase was in plug-flow. Also for the absorption and sulfuric acid catalyzed hydration of isobutene (Deckwer et al., 1977), it has been reported that conversions calculated from a simple model which treats the

Correspondence concerning this paper should be addressed to A. Varma.
D.T.-J. Huang is presently at Brookhaven National Laboratory, Upton, New York 11973.
0001-1541-81-4324-0111-$2.00.